The Deformation Mechanism of Fatigue Behaviour in a N36 Zirconium Alloy

Yingzhu Wang

Huanggang Middle School Guangzhou Branch
+86 18566395386
1476456993@qq.com

Abstract. Zirconium alloys are widely used as claddings in nuclear reactor. A N36 zirconium alloy has been deformed into a sheet with highly texture according to the result of electron back scatter diffraction test. Then this N36 zirconium alloy sheet has been cut into small beam samples with 12 x 3 x 3 mm^3 in size. In this experiment, a three-point bending test was carried out to investigate the fatigue behaviour of N36 zirconium alloy. Cyclic loadings were applied on the top middle of the beam samples. The region of interest (ROI) is located at the middle bottom of the front face of the beam sample where slip band was observed in deformed beam sample due to strain concentration by using scanning electron microscopy. Twinning also plays an important role to accommodate the plastic deformation of N36 zirconium alloy in fatigue, which displays competition with slip.

1. Introduction

Research into nuclear power began over 65 years ago, however, incidents such as the accident in Pennsylvania in 1979 and the disaster at Chernobyl in 1986 triggered increasing concern about the safety in nuclear industrial. There has been an increased use of zirconium alloys as fuel cladding within the nuclear industry since the late 1950s owing to a combination of their good corrosion resistance at operating temperatures and low neutron absorption. The cladding also protects the radioactive fuel from the surrounding environment whilst providing a good heat transfer surface. It is the value of the absorption cross-section that is most relevant for materials with nuclear uses.

Zirconium alloys used within the nuclear reactor are normally considered structural components, and their performance during operation is dependent on the deformation mechanisms that occur during operation and those that give rise to the final microstructure of the alloy as a result of the processing route. Deformation during operation normally involves elastic deformation, during which the material will return to its original shape, unless the material undergoes a stress which will lead to failure, as might occur during a loss of coolant accident (LOCA). During processing, the alloy normally undergoes a significant amount of plastic deformation which gives rise to the alloy's final microstructure and the mechanical properties it will exhibit during service. The deformation behaviour of zirconium alloys during processing and failure scenarios will be discussed in this section. Work done by Akhtar et al. [1] investigated the slip system operative for various crystallographic orientations and how these, along with a number of other conditions, effect the work hardening parameters. During this study, single crystal specimens were found to be most suitable when investigating deformation mechanisms under stress as the complex effects of grain boundaries do not have to be taken into consideration.

Twinning plays a significant role in the deformation of zirconium and zirconium alloys. Crystallographic twinning occurs when two separate crystals share some of the same crystal lattice points in a symmetrical manner. The preference type of twinning including the typical

shears and reorientations in zirconium has been concluded in previous research [2, 3] as shown in Fig. 1: $\{10\bar{1}2\}$ $<\bar{1}011>$ twinning and $\{11\bar{2}1\}$ $<\bar{1}\bar{1}26>$ twinning are activated when zirconium is under tensile stress along the direction of the c axis; when zirconium is under compression along the <c> direction $\{11\bar{2}2\}$ $<\bar{1}\bar{1}23>$ twinning and {1011} <1012> twinning are observed at room temperature and elevated temperatures, respectively.

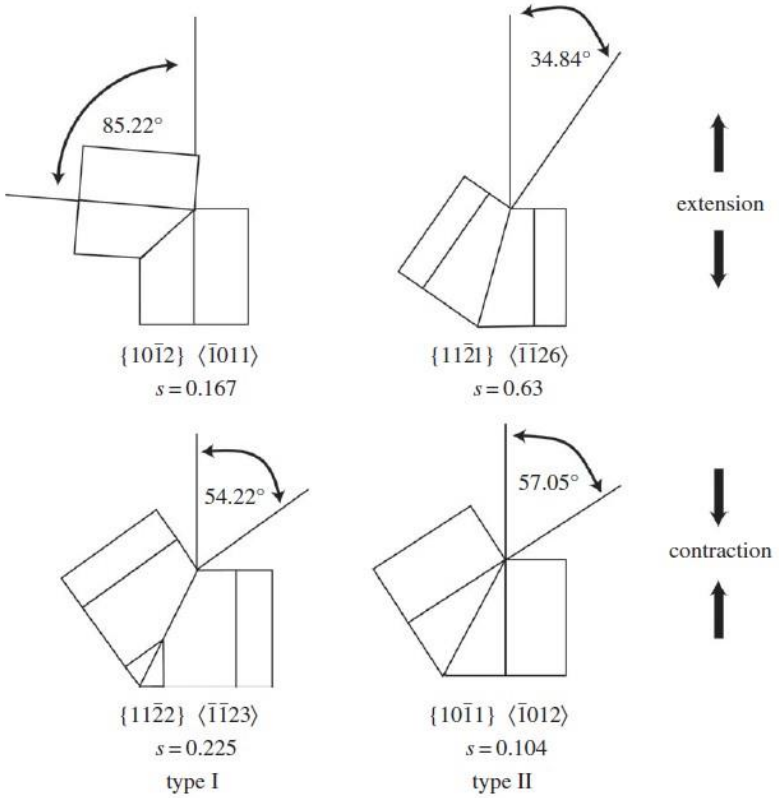

Figure 1. Twinning type in zirconium [2, 3].

Twinning causes a region within a parent grain which has a shear strain. This shear strain contributes to a crystallographic reorientation with respect to the parent crystal [3]. Twinning has a competition with slip during the deformation because twinning not only produces strains in the uniaxial extension or compression of the c axis, but also accommodates shears in the basal plane, and in the latter case twinning is the dominated mode [4]. Twinning contributes to the reorientatioin of the grain like slip, and it forms subgrains with different orientation compared with the matrix [5]. Kaschner et al [6] reported the effect of twinning on the hardening response in zirconium that twins influence the reload behaviour by either reorienting material for easy slip or by providing barriers to slip.

In this study, a three-point bending test was designed to investigate the deformation of N36 zirconium alloy. A finite element modelling was built up to estimate the deformation of N36 zirconium alloy. Additionally, high resolution digital image correlation (DIC) and electron backscatter diffraction (EBSD) technology were used to acquire the strain distribution and grain orientation in N36 zirconium alloy. These microstructure knowledge contributes to a deeper understanding of the deformation mechanism in zirconium. The relationship between slip and twinning has been discussed.

2. Methods and materials

2.1. Chemical composition of N36 alloy

The as-received material is a cold-rolled sheet of N36 alloy with the thickness at 3 mm. The chemical composition of N36 alloy is given in Table 1.

Table 1-1 Chemical composition of N36 alloy

Element	Sn	Fe	Cr	O
Percentage (%)	1.45	0.27	0.10	0.09

2.2. Three-point bending test

The as-received sheet of N36 alloy has been cut into beam samples with 12 × 3 × 3 mm^3 in size as shown in Fig. 2(a). These samples were then deformed in a three-point bending test on a Zwick machine by applying cyclic loading. The schematic diagram of the three-point bending is shown in Fig. 2(b). The force-controlled cyclic loading was applied on the top middle of beam. Two cylinder pins were fixed to support the beam in the bending test, which make the beam not free at vertical direction. In beam theory, stress is expected to concentrate at middle bottom of beam which is marked in red. Thus, the region of interest (ROI) is focused at this red section. The loading history is plotted in Fig. 2(c).

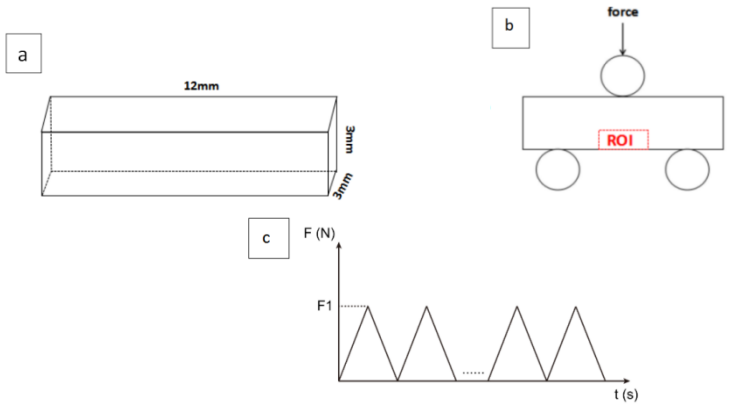

Figure 2. Schematic diagram of three-point bending test (a) three-point bending test setting; (b) the size of beam sample; (c) loading history of cyclic loading

2.3. High-resolution digital image correlation (HR-DIC)

Digital image correlation (DIC) technology was developed to measure the strain distribution in the ROI during the three-point bending. The basic method of DIC is to measure the displacement change by tracking the characteristic on the surface of the sample. In this experiment 250 nm particles of diamond were sprayed on the sample surface forming a uniform distribution of spot coating as shown in Fig.3. After each loading increment, the beam sample was removed from three-point bending rig to Sigma 300 Scanning Electron Microscopy (SEM). The morphology of the speckle coating was observed by SEM. Based on a cross-correlation method by an in-house coding the strain distribution of deformation in beam was obtained.

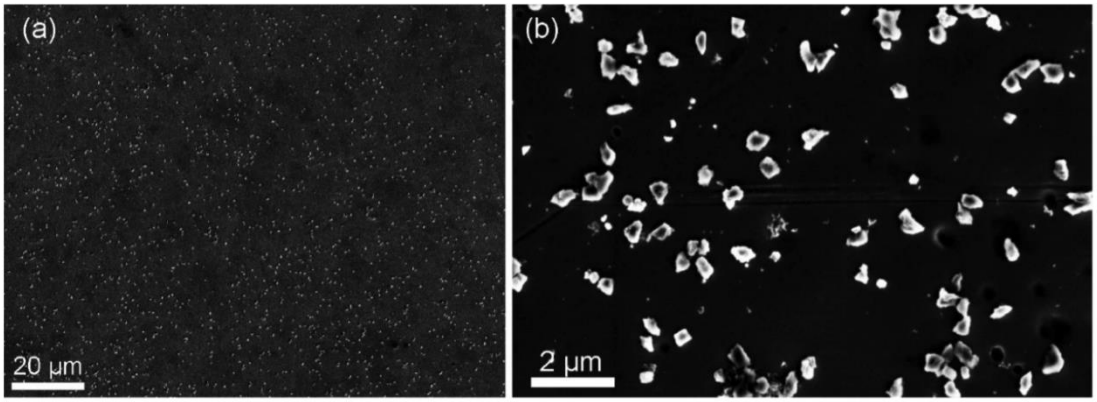

Figure 3. Particles sprayed on the surface of the sample for DIC measurement. (a) low magnification image; (b) high magnification image

2.4. EBSD and High-resolution EBSD

Electron backscatter diffraction (EBSD) is a technique for automatically obtain information about crystallographic orientation from samples at each individual scanning point in a SEM. The Zeiss Auriga-40 SEM and Bruker EBSD detector was used to observe the free surface of samples in this experiment. EBSD is not only used to measure the texture, ODF and MODF in materials, but also can be used to analysis the phase composition by checking Kikuchi pattern.

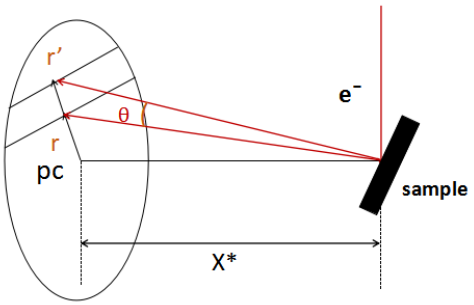

Figure 4. Schematic of EBSD showing the band width relation

Fig. 4 shows the Fundamental of EBSD. The samples in the EBSD test were tilted by 70 degrees from the horizontal plane. The incident electrons that satisfy the Prague law cast the crystal face onto the screen forming the Kikuchi band. The width of the bands is a direct function of the d-spacing of the diffracting plane through Bragg's law:

$$\lambda = 2d_{hkl}sin\theta,$$

λ is the wavelength of the incident wave, d_{hkl} is the d-spacing of the reflection plane, and θ is the angle prescribing the width of the corresponding Kikuchi band.

3. Finite element modelling

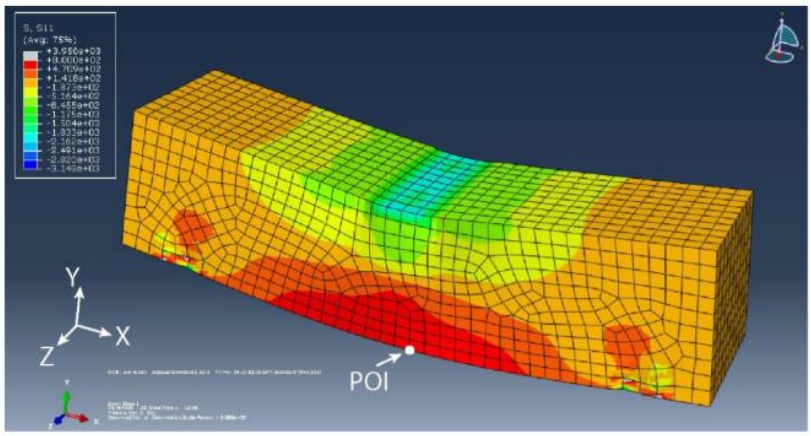

Figure 5. Three-point bending finite element simulation of N36 zirconium alloy beam

Fig 5 shows the simulation of the stress distribution of a zirconium alloy beam during a three-point bending test. This beam was applied by a cyclic loading of a magnitude of 1300 N at the middle top. This beam was placed in a special three-point bending setting where it was supported by two cylinder pins. In this way there has no freedom for the beam to move in the vertical direction but it only can be moved in the horizontal direction. The point of interest (POI) is located at the middle bottom of the beam shown as white point in the figure. From the simulation results it can be seen that the stress at POI is the highest at 800 MPa during deformation compared with the surrounding region. In the area around the POI, the farther away from the POI the smaller the stress value is. The stress also highly concentrated at the area close to the two supporters. However, since the positions of the two supporters are far away from the POI the stress distribution at the POI is not affected.

4. Results and discussion

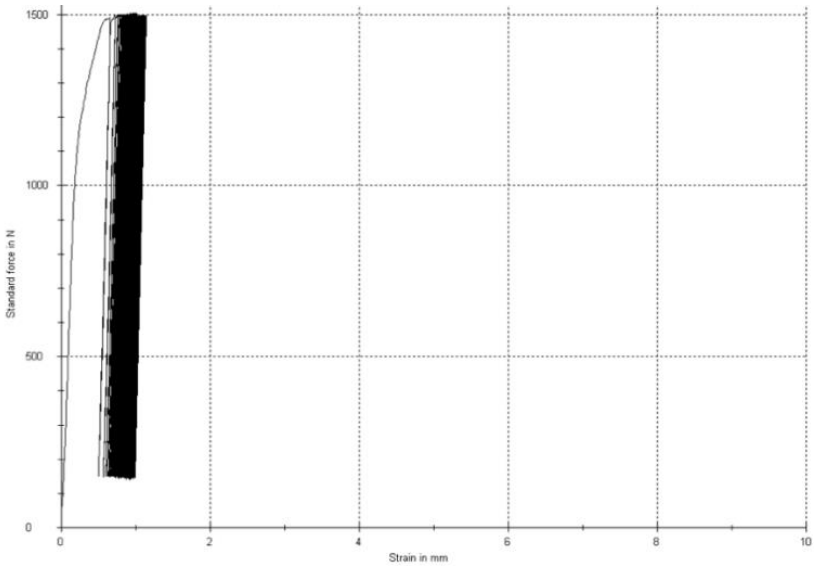

Figure 6. Force versus displacement (strain in mm) curve of cyclic loading test

Fig.6 shows the relationship between applied force (standard force) and displacement (strain in mm) during a cyclic loading. The maximum applied force is 1500N and the minimum one is 150 N with the ratio, R = 0.1. At the first cycle the alloy shows obvious plastic deformation with displacement remains around 0.5 mm after unload. After that, the displacement increases

at every cycle. However, the increase value of displacement of every cycle reduces progressively. After 100 cycle, the increment of displacement of every cycle is relatively low but the total accumulation is pretty large which reaches 1 mm at 2000 cycle.

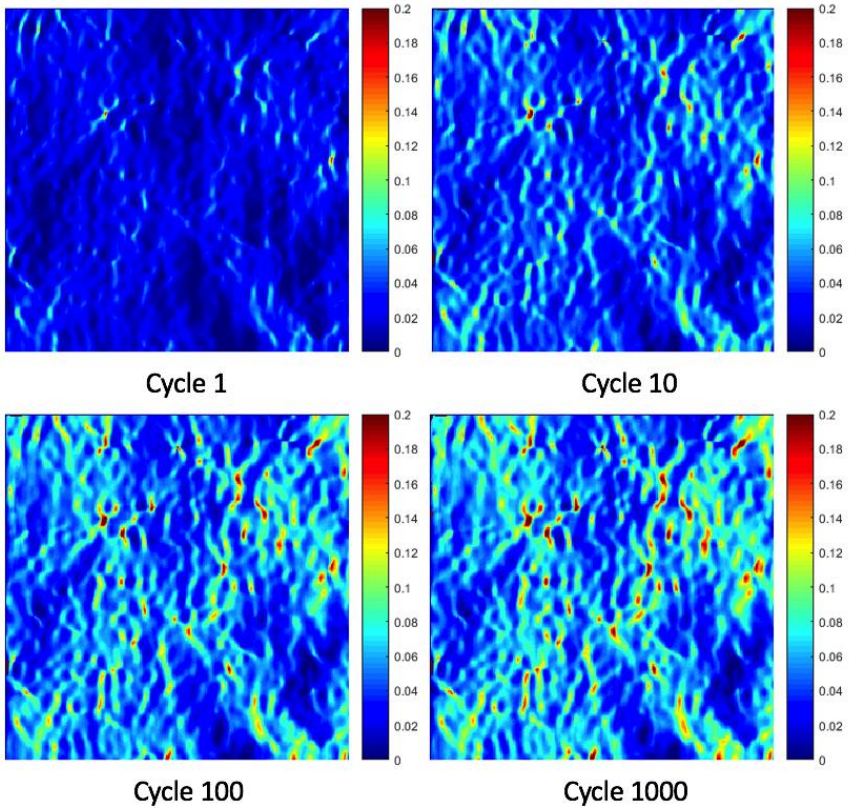

Figure 7. DIC results of three-point bending N36 alloy showing the strain distribution in the area of interest

Fig 7 illustrates the DIC result of alloy during the three-point bending cyclic loading. These DIC results give the total distribution of cycle 1, cycle 10, cycle 100 and cycle 1000 at the region of interest. The strain shows apparently localization in the grain or at the grain boundary. From cycle 1 to cycle 10, the strain localization enhances obviously with the maximum strain reaches 0.2. After the cycle 10, the strain increases continuously but shows not much difference between cycle 100 and cycle 1000.

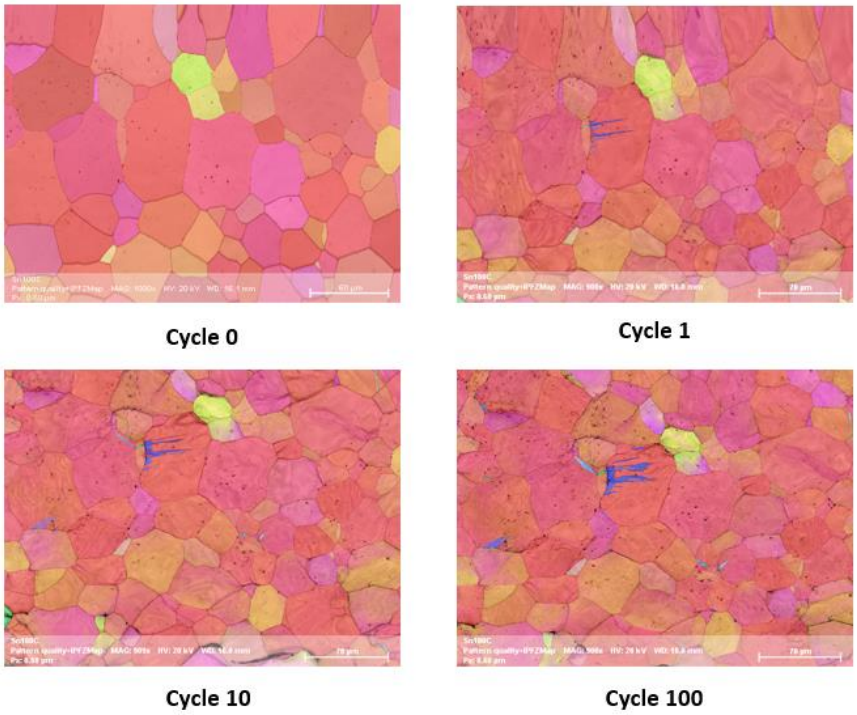

Figure 8. EBSD results of cyclic loading three-point bending test

Fig 8 shows the EBSD results of N36 alloy applied by cyclic loading from cycle 0 to cycle 100. The observation on the surface of electropolished sample gives a satisfactory view on the orientation variation of grains in the region of interests, which indicates a strong basal texture in this sample. The grain size ranges from 10 μm to 50 μm. The deformed grains represent shape variation and lattice distortion, which contributes to the formation of subgrains. In cycle 0, the original situation of the grains shows no twinning or slip band. However, twinning, marked as blue area, appears from cycle 1 and enhances with the increase of cycle number. Meanwhile, only a few slip bands can be seen in the grain but it does not dominate the deformation. It indicates that twinning is necessary for the deformation of this alloy.

5. Conclusion

Three-point bending test on beam samples combining with finite element modelling analysis and experimental method was carried out to investigate the deformation of N36 zirconium alloy. The conclusions below have been obtained:

(1) The modelling results indicates that the stress peaked at the middle bottom of the beam sample.

(2) Strain localization was observed in N36 zirconium alloy during the cyclic loading three-point bending test which indicates the localization of slip band or the existence of twinning.

(3) Twinning dominates the deformation of N36 zirconium alloy applied at three-point bending test displaying competition with slip according the analysis on EBSD results.

6. References

[1] A. Akhtar, Teghtsoo.A, Acta Metallurgica, 19 (1971) 655-&.
[2] E. Tenckhoff, Deformation Mechanisms, Textures, and Anisotropy in Zirconium, 1988.
[3] T.B. Britton, F.P.E. Dunne, A.J. Wilkinson, Proceedings of the Royal Society A: Mathematical, Physical and Engineering Science, 471 (2015) 20140881.
[4] C.N. Tome, R.A. Lebensohn, U.F. Kocks, Acta Metall Mater, 39 (1991) 2667-2680.
[5] B. Clausen, C.N. Tomé, D.W. Brown, S.R. Agnew, Acta Materialia, 56 (2008) 2456-2468.
[6] G.C. Kaschner, C.N. Tomé, I.J. Beyerlein, S.C. Vogel, D.W. Brown, R.J. McCabe, Acta Materialia, 54 (2006) 2887-2896.